
Article:
Cheng, VWT orcid.org/0000-0003-4159-8697, Soto, MS, Khrapitchev, AA et al. (5 more authors) (2019) VCAM-1-targeted MRI Enables Detection of Brain Micrometastases from Different Primary Tumors. Clinical Cancer Research, 25 (2). pp. 533-543. ISSN 1078-0432

https://doi.org/10.1158/1078-0432.CCR-18-1889

Supplementary Methods

Antibody conjugated-MPIO synthesis

1μm diameter MPIO (Dynabeads MyOne Carboxylic Acid; ThermoFisher Scientific) were chemically treated with 1-Ethyl-3-(3-dimethylaminopropyl)carbodiimide (EDC; ThermoFisher Scientific) to yield amide bonds as antibody binding sites. Activated carboxy-MPIO were incubated overnight with 80μg of rat anti-mouse VCAM-1 low endotoxin/azide-free antibody (cat. no. 1510-14; Cambridge Bioscience) under continuous agitation at room temperature. Rat IgG1 isotype control low endotoxin/azide-free antibody (cat. no. 0116-14; Cambridge Bioscience) was used for control IgG-MPIO. Successful antibody loading (~20,000 antibodies per MPIO) was confirmed via fluorescence-activated cell sorting, compared against standardised calibration beads.

Immunohistochemistry and immunofluorescence: Mouse tissue

After MRI, animals were transcardially perfused under terminal anaesthesia with 0.9% heparinised saline followed by 50ml of periodate lysine paraformaldehyde containing 0.1% (vol/vol) glutaraldehyde. The brains were post-fixed, cryoprotected, embedded, and frozen in isopentane at −20°C, before cryosectioning into 10μm coronal slices. Immunohistochemical analysis was performed to determine tumour number and area, VCAM-1 expression and MPIO binding. All incubations were performed at room temperature, unless otherwise stated.

For immunohistochemical detection of MDA231Br-GFP and SEBTA-001 tumours, 10μm sections were quenched with 0.3% hydrogen peroxide in methanol (Sigma Aldrich) and blocked as per the Mouse-on-Mouse kit protocol (Vector Laboratories) for 1h. Sections were incubated with primary

mouse anti-human cytokeratin antibody (12.5µg/ml; cat. no. 345779; BD Biosciences) overnight at 4°C. Subsequently, the sections were washed using PBS, and then incubated with a biotinylated horse anti-mouse IgG secondary antibody (1:200; cat. no. BA-2001; Vector Laboratories) for 1h. Slides were washed and then incubated in Vectorelite ABC kit (1:1:100; Vector Laboratories) for 45min. The peroxidase was visualized using 3,3'-diaminobenzidine (DAB; Sigma Aldrich). Sections were counterstained with 0.05% (vol/vol) cresyl violet (Sigma Aldrich) in distilled water. For H1_DL2 tumours, the protocol was modified through 10% normal goat serum blocking for 1h, overnight incubation with primary rabbit anti-human melan A antibody (1:100; cat. no. ab51061; Abcam) at 4°C and then incubation with biotinylated goat anti-rabbit IgG secondary antibody (1:100; cat. no. BA-1000; Vector Laboratories) for 1h.

For immunohistochemical detection of VCAM-1, sections were incubated overnight at 4°C with the primary rat anti–mouse VCAM-1 antibody (10µg/ml; Southern Biotech). After rinsing with PBS, sections were incubated for 1h with a biotinylated goat anti-rat IgG secondary antibody (1:100; Vector Laboratories). VCAM-1 staining was detected using a standard DAB reaction, and sections were counterstained with cresyl violet.

For immunofluorescent co-localisation of tumour-associated blood vessels and VCAM-1, sections were quenched with 0.3% (vol/vol) hydrogen peroxide in methanol and then sequentially streptavidin- and biotin-blocked (SP-2002; Vector Laboratories) for 15min, followed by 1h incubation in Tris·NaCl blocking buffer (TNB; PerkinElmer). Sections were incubated overnight at 4 °C with the primary rat anti–mouse VCAM-1 antibody (10µg/ml; Southern Biotech) and primary goat anti-mouse CD31 antibody (2µg/ml; cat. no. AF3628; R&D Systems) in TNB. In addition, the sections were incubated

with antibodies targeting tumour specific markers as follows: primary chicken anti-GFP antibody (1:50; cat. no. ab13970; Abcam) for MDA231Br-GFP, primary rabbit anti-human (1:100; cat. no. ab51061; Abcam) for H1_DL2 and primary mouse anti-human TTF-1 (1:50; cat. no. ab72876; Abcam) for SEBTA-001. After rinsing with PBS, slides were incubated with a corresponding biotinylated IgG secondary antibody against the tumour specific marker antibody (1:100; Vector Laboratories) in TNB for 30min, washed with PBS, incubated with streptavidin-HRP (1:200; Perkin Elmer) in TNB for 30min, washed, and incubated for 8min in the dark with tyramide signal amplification–biotin (1:100; Perkin Elmer) in dilution buffer. Slides were washed and incubated with a streptavidin-488 fluorophore (1:100; cat. no. SA-5488; Vector Laboratories), a secondary donkey anti-rat Dylight 405 fluorophore (1:100; cat. no. 712-476-150-JIR; Stratech) and a secondary rabbit anti-goat 555 fluorophore (1:100; cat. no. A-21431; Invitrogen) for 1h. MDA231Br-GFP sections were incubated with a secondary donkey anti-chicken CF 488A (1:100; cat. no. SAB4600031; Invitrogen) fluorophore Slides were cover-slipped using Vectashield mounting medium.

Images were acquired using a confocal microscope (Leica TCS SP8 Confocal platform; Leica Microsystems) and analysed using ImageJ (rsbweb.nih.gov) and Leica Application Suite X (Leica Microsystems) software. Detection ranges were set to eliminate cross-talk between fluorophores: 409–485 nm for DAPI, 494–553 nm for Alexa Fluor 488, and 564–712 nm for Alexa Fluor 555.

Quantitation of tumour volume and VCAM-1 expression

Alternate sections for each brain were stained immunohistochemically with tumour-specific markers. Histological slides were digitally scanned on an Aperio CS2 Brightfield scanner (Leica Biosystems) at x20 magnification. The digital images were visualised using Imagescope (v.12; Leica

Biosystems) software and manually annotated to outline individual tumours on each section as a region of interest (ROI). The tumour area was returned for each ROI, in μm^2, and missing data for the remaining alternate sections were calculated by linear interpolation. The sum of the tumour areas was multiplied by the slice thickness (10µm) to determine the total volume of tumours in each brain, reported in mm^3.

To quantify VCAM-1 expression in each brain, alternate sections were immunohistochemically stained for VCAM-1 and digitally scanned on an Aperio CS2 Brightfield scanner (Leica Biosystems) at x20 magnification. The digital images were visualised using Imagescope (v.12; Leica Biosystems) software and manually annotated to outline the entire section as a region of interest, excluding the choroid plexus and ventricles as these are known sites of false positive staining. Using the in-built Positive Pixel Count v.9 algorithm, all medium and strong intensity brown pixels (Intensity threshold between 0 to 174, intensity threshold of negative pixels = -1, Colour saturation threshold = 0.04, Hue width = 0.5) were summed for each section and divided by the total area of the corresponding ROI to determine the VCAM-1 staining, reported as number of positive pixels per mm^2 of brain.

Immunohistochemistry: Human tissue

Three representative cases of human brain metastasis were obtained for each tumour type, as previously described (1); breast cancer, lung adenocarcinoma and melanoma (Walton Research Tissue Bank reference: 11/WNo03/02). Together with one VCAM-1 positive control brain sample (nonspecific inflammation), the samples were examined to assess VCAM-1 up-regulation; 6µm thick sections were cut from paraffin-embedded, formalin-fixed surgical material and processed. For immunohistochemistry, sections were dewaxed, rehydrated, and quenched. Blocking was achieved with 10% normal goat serum in PBS. A rabbit anti-human VCAM-1 primary antibody (20µg/100µl; Santa

Cruz Biotechnology) was used, followed by biotinylated goat anti-rabbit IgG secondary antibody (1:200; Vector Laboratories) and visualized with DAB substrate as the chromogen. Sections were counterstained with cresyl violet in distilled water.

Histological slides were digitally scanned on an Aperio CS2 Brightfield scanner (Leica Biosystems) at x20 magnification and analysed using Imagescope (v.12; Leica Biosystems) software for assessment of VCAM-1 vessel proximity to tumour edge.

Supplementary Figures

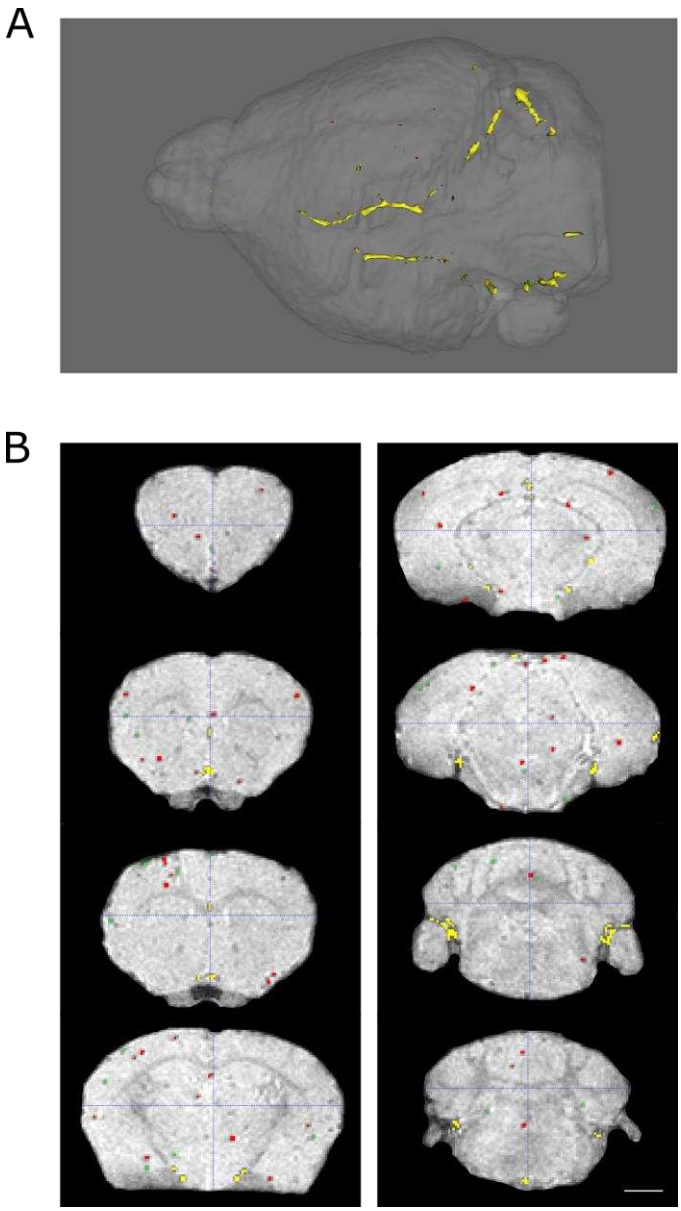

Supplementary Figure S1. (A) 3D reconstruction of a representative post-processing mask of a mouse brain with MDA231Br-GFP metastases following intravenous injection of VCAM-MPIO showing segmented hypointense regions classified by colour: green (1 voxel), red (between 2 and 19 voxels) and yellow (≥20 voxels). **(B)** The post-processing mask was overlaid on the corresponding *T*2*-weighted images to verify the accuracy of the analysis; scale bar = 1.5mm.

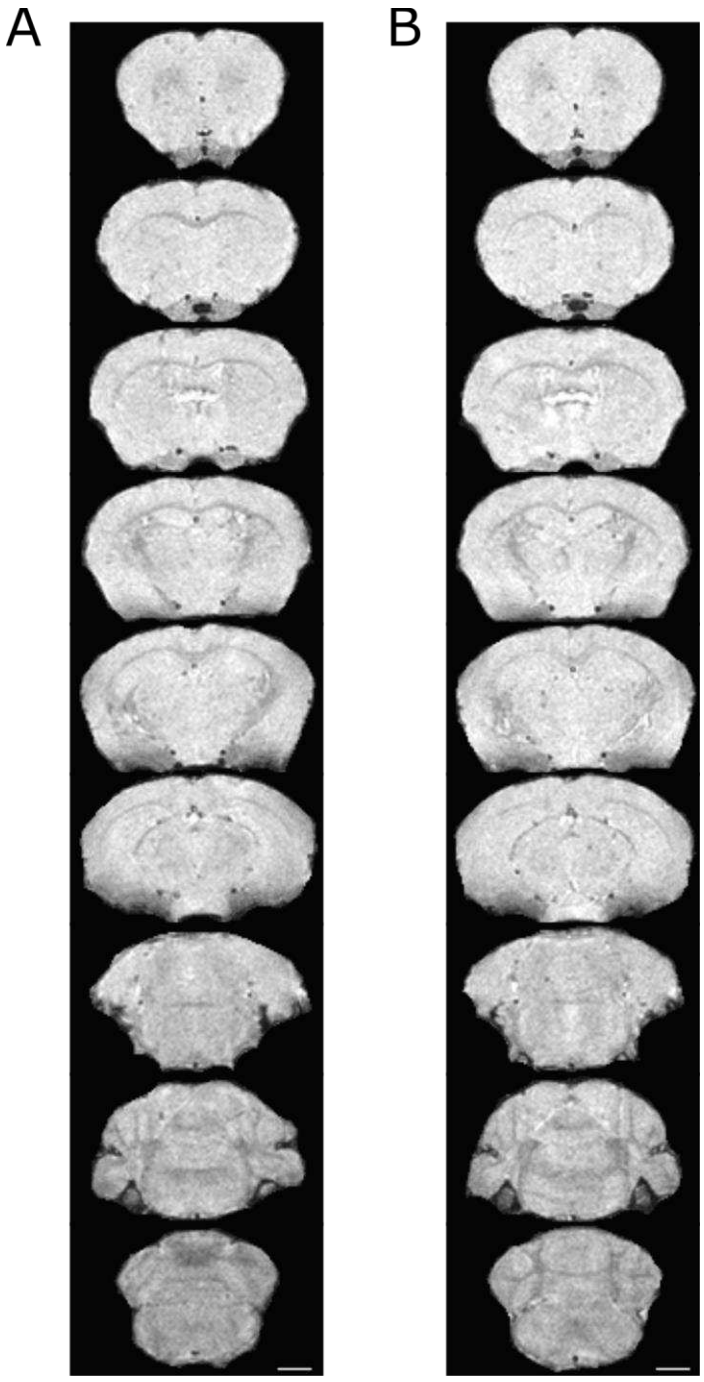

Supplementary Figure S2. Selected T_2^*-weighted images from **(A)** a naïve mouse following intravenous injection of VCAM-MPIO and **(B)** a mouse bearing MDA231Br-GFP metastases following intravenous injection of IgG-MPIO; scale bar = 1.5mm. Minimal background (non-specific) hypointensities are evident.

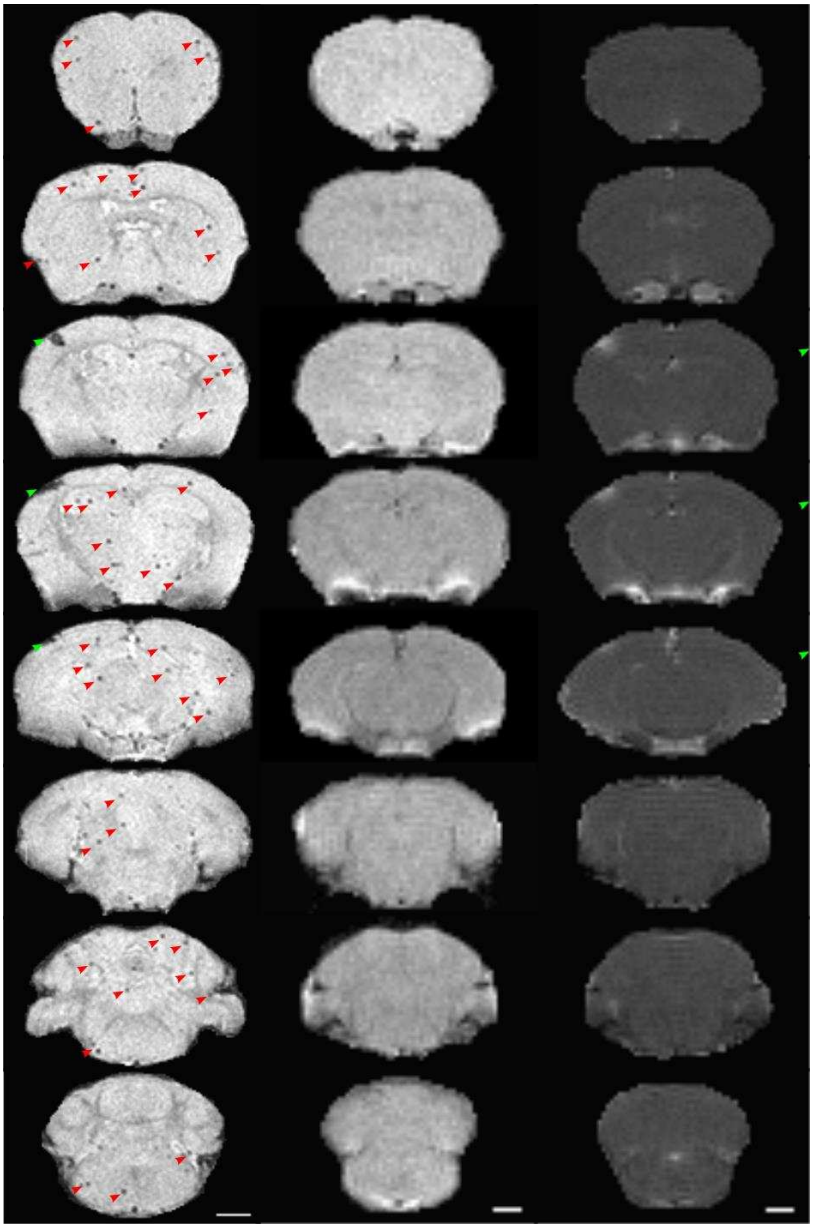

Supplementary Figure S3. Representative T_2^*-weighted images (left-hand column) and corresponding pre- (middle column) and post-gadolinium (right-hand column) T_1-weighted images for a mouse injected intracardially with SEBTA-001 cells; scale bar = 1.5mm. Gadolinium enhancement confirms presence of a single large metastasis exhibiting blood-brain barrier breakdown (green arrow). The presence of additional micrometastases is indicated on the T_2^*-weighted images as multiple focal hypointensities (red arrows), which are not detected on the post-contrast T_1-weighted images.

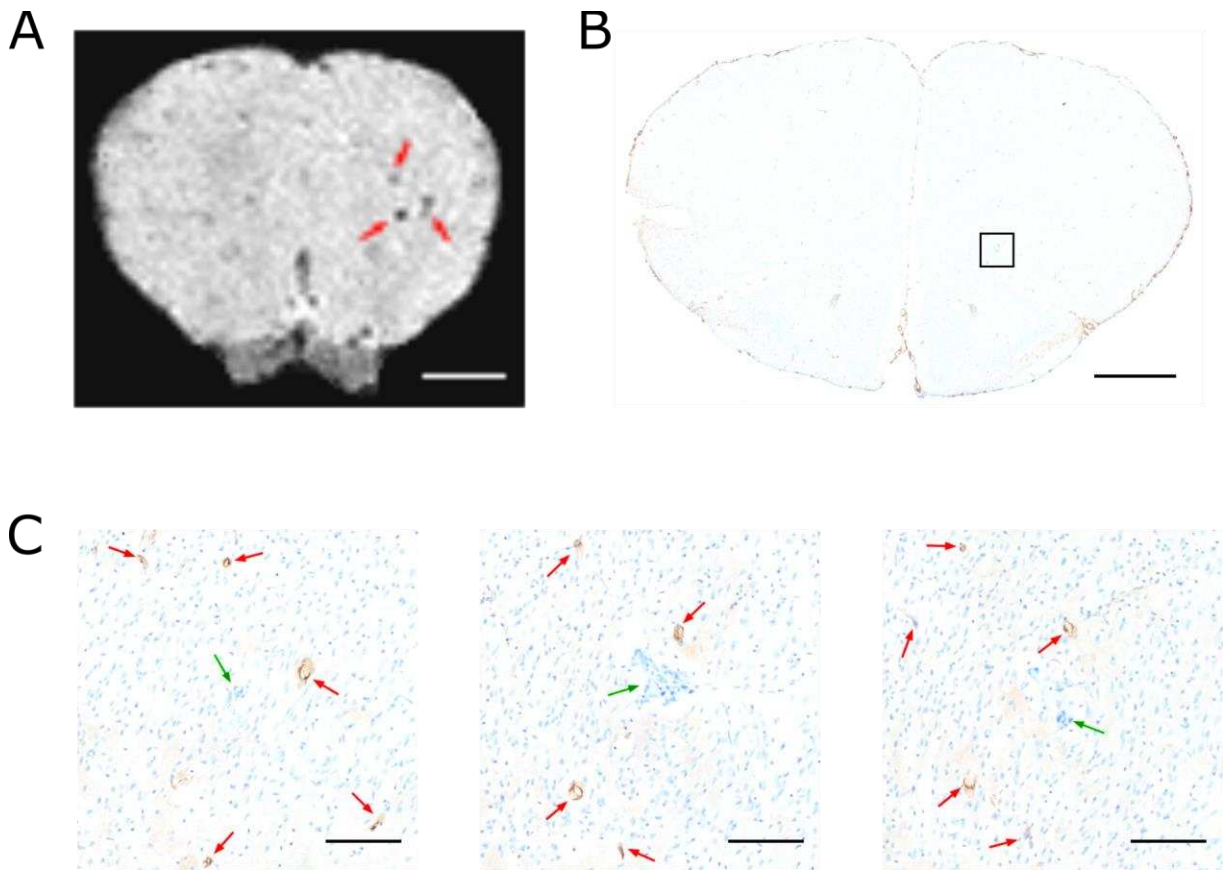

Supplementary Figure S4. (A) Axial T_2^*-weighted image slice of a mouse brain following intracardiac injection of SEBTA-001 cells with several hypointensities (red arrows); scale bar = 1.5mm. (B) One corresponding histological section of the same mouse demonstrating a single SEBTA-001 metastasis in this location (black box); scale bar = 1.5mm. (C) Magnified images from alternate sections of the highlighted metastasis showing multiple VCAM-1 activated vessels (red arrows) around the periphery of the tumour (green arrows); scale bar = 100µm.

1. Zakaria R. Investigation of local brain invasion by cerebral metastases and implications for clinical management. University of Liverpool Repository: University of Liverpool; 2016.